lubricants

MDPI

Article

Resistance to Wear during Friction without Lubrication of Steel-Cast Iron Pairing with Nanocrystalline Structure-Reinforced Surface Layers

Ihor Hurey [1,2], Pavlo Maruschak [3,*], Andy Augousti [4], Alan Flowers [4], Volodymyr Gurey [1], Volodymyr Dzyura [3] and Olegas Prentkovskis [5]

[1] Department of Robotics and Integrated Mechanical Engineering Technologies, Lviv Polytechnic National University, 12, Bandera St., 79013 Lviv, Ukraine; ihor.v.hurei@lpnu.ua (I.H.); volodymyr.i.hurei@lpnu.ua (V.G.)
[2] Faculty of Mechanics and Technology, Rzeszow University of Technology, 12, Powstancow Warszawy St., 35-959 Rzeszow, Poland
[3] Department of Wheel Vehicles, Ternopil Ivan Puluj National Technical University, 56, Ruska St., 46001 Ternopil, Ukraine; volodymyrdzyura@gmail.com
[4] Faculty of Engineering, Computing and the Environment, Kingston University London, London SW3 15DW, UK; augousti@kingston.ac.uk (A.A.); a.flowers@kingston.ac.uk (A.F.)
[5] Department of Mobile Machinery and Railway Transport, Vilnius Gediminas Technical University, Plytines g. 27, LT-10105 Vilnius, Lithuania; olegas.prentkovskis@vilniustech.lt
* Correspondence: maruschak.tu.edu@gmail.com

Abstract: During the TDT of 41Cr4 steel specimens, a uniformly reinforced white layer with a nano-crystalline structure is formed in the surface layers. The wear resistance of sliding friction without the lubrication of a pair of steel 41Cr4—grey cast iron EN-GJL-200 (EN) under the face-to-face ("ring-ring") scheme has been studied. It is revealed that when the sliding velocity changes from 0.25 m/s to 4 m/s and the unit load changes from 0.2 MPa to 1.0 MPa, a pair with a reinforced surface layer on 41Cr4 steel specimens and unreinforced specimens of EN-GJL-200 (EN) grey cast iron has a higher wear resistance than an unreinforced pair. The wear resistance increases for both reinforced and not reinforced specimens operating in a friction pair.

Keywords: white layer; wear; nanocrystalline structure; thermo-deformation treatment

Citation: Hurey, I.; Maruschak, P.; Augousti, A.; Flowers, A.; Gurey, V.; Dzyura, V.; Prentkovskis, O. Resistance to Wear during Friction without Lubrication of Steel-Cast Iron Pairing with Nanocrystalline Structure-Reinforced Surface Layers. *Lubricants* **2023**, *11*, 418. https://doi.org/10.3390/lubricants11100418

Received: 14 August 2023
Revised: 21 September 2023
Accepted: 22 September 2023
Published: 24 September 2023

1. Introduction

The reliability of products (technological equipment) depends on the quality of the individual machine parts that comprise them and is determined by their operating characteristics. The operating characteristics of machine parts are determined by the physico-chemical and mechanical properties of the surface layer, as well as the quality parameters of the working surfaces of the parts, which are formed during the finishing operations of the manufactured parts [1]. The quality parameters of the machined surface and surface layer have a major impact on the operating characteristics of machine parts [2], namely resistance to fatigue fracture [3], wear [4–6], corrosion [7], etc. All fracture processes that occur during product use start at the surface [8].

The surface layer wears in the process of the sliding friction of the contacting surfaces of machine parts. The actual contact area, local stress, contact stiffness, oil film formation conditions, and other parameters have a significant effect on the contact interaction of machine part surfaces [9,10]. The wear resistance and contact strength of surface layers depend mainly on the quality parameters of the layer, such as its thickness, microhardness, magnitude and sign of residual stresses, structure, texture, grain size, etc. [4,6,11].

New methods of the surface treatment of the working surfaces of machine parts can improve the operating characteristics and performance parameters of components and

products in general [9]. Such methods allow the formation of the specified surface stereometry parameters (waviness, roughness, linear and surface bearing capacity profile) and the corresponding characteristics (hardness, residual stress, structure, phase and chemical composition, texture, etc.) of the working surfaces of machine parts. They mainly affect the processes of friction and wear, fatigue, corrosion, and fatigue destruction [1,3,7,9]. It is sufficient to strengthen only the surface layers of the contacting surfaces of machine parts to improve the operating characteristics of machine parts [1,12]. The formation of reinforced surface layers on the working surfaces of machine parts and ensuring the appropriate accuracy and quality of machined surfaces are problematic tasks. For this purpose, various cutting methods are used, which provide high parameters of accuracy and quality of treated surfaces [13], the formation of a regular profile on the contacting surfaces [14], grinding with various types of abrasive wheels [15], surface plastic deformation [16], the application of various coatings [17–19], surfacing with alloy metal [20,21], electrophysical and electrochemical processing methods [22], etc. [23].

In order to strengthen the surface layers of the working surfaces of machine parts, which in most cases work under frictional conditions, processing methods using concentrated energy sources are used [24,25]. These include laser [26], plasma, ion-beam [27], friction [28,29], and other treatments [30]. In the process of these treatments, concentrated sources of thermal energy act on local volumes of metal in the surface layer of the treated surfaces. The metal is heated at a high rate to temperatures above the phase transformation point. After the removal of the heat source, the heated local volume of metal cools at a high rate. By heating and cooling local volumes of metal at high rates, strengthened (hardened) layers (white layers) with a nanocrystalline structure (NCS) are formed in the surface layers [31,32]. The surface layers with an NCS have a fine-grained structure, altered phase and chemical compositions [33], as well as specific physical, mechanical, electrochemical, and other properties that differ significantly from the base metal [30,34]. The resulting strengthened layers significantly improve the performance of the working surfaces of machine parts [35]. Methods involving intense plastic deformation are used to grind grains, increase hardness, and modify properties [36,37]. The process of using these methods involves intensive grain grinding and metal formation with an NCS [38,39].

A metal with an NCS significantly improves its operating characteristics [40]. Thermodeformation treatment (TDT) is a method of reinforcing the working surfaces of machine parts. This treatment combines two methods: the action of a highly concentrated energy source and the intense plastic deformation of the metal of the surface layer of the treated surfaces [41,42]. A highly concentrated energy source arises in the process of the high-speed friction (60–90 m/s) of the tool on the treated surface in the contact zone [43,44]. The local contact zone is heated at a high rate (5×10^5–4×10^6 K/s) to temperatures above the phase transition point of the metal being processed [45]. In the contact zone, the shear deformation of the surface layer metal occurs. The tool is made with transverse grooves on its periphery (with a discontinuous working surface), which interrupts the action of thermal energy and increases the intensity of shear deformation [46]. Due to the movement of the contact zone along the treated surface, the local zone of the metal surface layer is cooled at a high rate (2×10^5–1×10^6 K/s) [45]. Strengthened surface layers with an NCS (white layers) are formed on the treated surfaces of machine parts [47,48].

The aim of this work was to study the effect of surface layer reinforcement with an NCS on the wear resistance of a friction pair of steel 41Cr4—grey cast iron EN-GJL-200 (EN) during friction without lubrication.

2. Materials and Methods

The flat surfaces of the specimens were strengthened by using TDT on a grinding machine KNUTH HFS 3063 VS (Wasbek/Neumünster, Germany) (Figure 1). The DC electric motor with driver were installed on the spindle rotation drive to achieve the required speed on the peripheral working surface of the tool (60–90 m/s). The research was carried out at a speed of 70 m/s.

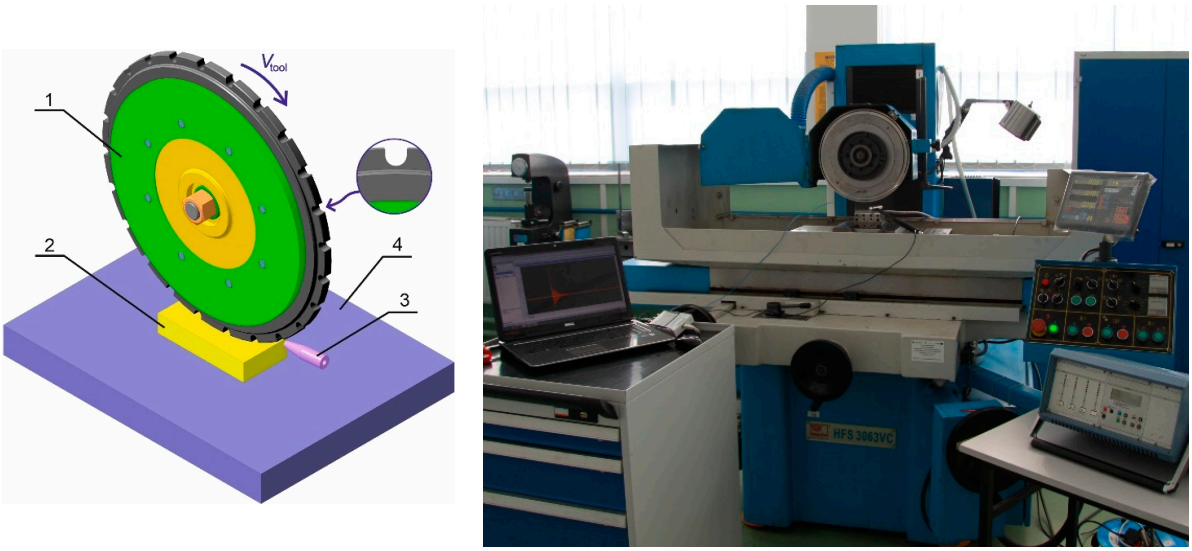

(**a**) (**b**)

Figure 1. Scheme (**a**): 1—tool; 2—sample; 3—nozzle (to direct liquid medium to the treatment zone); 4—table of grinding machine; V_{tool}—linear speed of the tool; (**b**) equipment for TDT of flat surfaces.

The tool was made of X10CrNiTi18-10 (EU) stainless steel in the form of a disk. The diameter of the tool was 360 mm (the same as the diameter of the grinding wheel it was installed in place of), and the width of the working surface was 6–8 mm. The disk was mounted on a faceplate used on this machine. The faceplate with the attached disk was statically balanced before being mounted on the machine.

The tool with a smooth working surface (tool-SWS) and transverse grooves (tool-TTG) on its working surface was used for the TDT (Figure 1). The transverse grooves (24 pcs.) alternated evenly with the smooth surface. The groove width was 12 mm. The tool was pressed against the treated surface with a force of 1000 N. Under the action of the pressure force, intense friction occurs in the zone of contact, which is a source of highly concentrated thermal energy and a generator of the intense plastic deformation of the surface metal layer of the treated surfaces. When the groove passes over the zone of contact between the tool and the workpiece, the workpiece is unloaded and the heat flow is stopped. When the next smooth surface comes into contact, the contact zone is sharply loaded, and its longitudinal deformation is intensified. A strengthened layer is formed in the surface metal layer of the treated surfaces.

The process medium is supplied to the processing zone during the TDT. Mineral oil with active additives containing polymers was used as a technological medium. In the process of TDT, under the influence of high temperatures and pressures in the tool-part contact zone, the process medium decomposes into its constituent chemical elements and diffuses into the metal surface layer. The chemical composition of the metal of the surface layer of the machined surfaces changes [49].

The wear resistance of the studied pair of steel 41Cr4—grey cast iron EN-GJL-200 (EN) was determined during friction without lubrication on a friction machine of the UMT-1, according to the scheme "ring-ring" (Figure 2). The tested specimens are shown in Figure 3. The sliding velocity varied from 0.2 m/s to 4 m/s. The load on the contacting surfaces of the specimens was adjusted in the range from 0.1 MPa to 1.5 MPa. The counter-specimen was mounted in a differential sensor of a force meter, the signal from which recorded the friction moment of a given pair. Three thermocouples with a diameter of 0.2 mm were mounted on it. The signals from the thermocouples were recorded using an automatic three-channel potentiometer. The integral temperature was recorded at a depth of 0.3–0.5 mm below the friction surface.

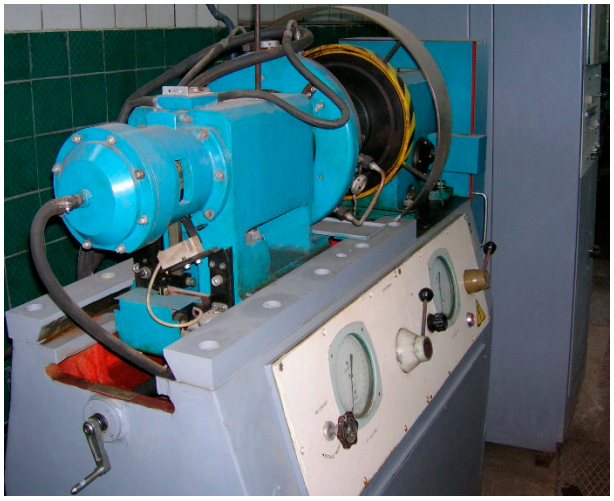

Figure 2. General view of the universal friction equipment (UMT-1) to determine the wear resistance during sliding friction.

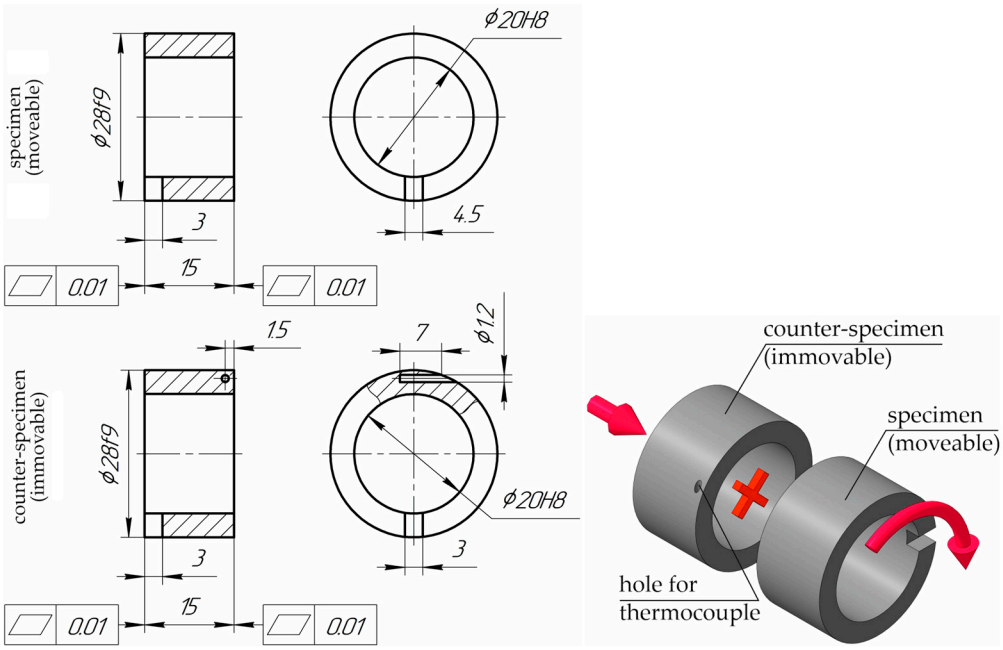

Figure 3. Sketch of specimen and counter-specimen for the study of sliding friction wear according to the "ring-ring" scheme.

The contacting face surfaces of the friction pair specimens were run-in before the tests. The run-in was performed until the friction torque stabilized and the face surfaces of each specimen were fitted. The contact area was at least 90% of the area of each sample.

The moving specimens of the friction pairs under study were made of steel 41Cr4 (quench hardening (QH) and low-temperature tempered (LTT), HRC 48–51), and the counter-specimens (immovable) were made of grey cast iron EN-GJL-200 (EN). The working face surfaces of the movable specimens were reinforced by TDT with a tool-SWS and a tool-TG. The counter-specimens were not reinforced, only ground. For comparison, a friction pair was used in which the moving specimens were not strengthened.

The chemical composition of the steel 41Cr4 is as follows: mass. %: 0.40 C; 0.78 Mn; 0.26 Si; 1.12 Cr; 0.01 S; 0.01 P; and Fe: balance. The chemical composition of the cast iron EN-GJL-200 is as follows: mass. %: 3.4 C; 0.85 Mn; 1.9 Si; 0.15 S; 0.2 P; and Fe: balance.

The roughness of the working surfaces of the specimens after TDT was Ra = 0.35–0.50 μm with a tool-SWS, Ra = 0.25–0.40 μm with a tool-TG, and Ra = 0.50–0.63 μm after grinding.

The amount of wear of each specimen was determined by the loss of their mass after each stage of friction, which was determined by weighing on the lab analytical balance (accuracy ± 0.2 mg). The wear intensity of the friction pair specimens was determined by the amount of their wear.

The value of the average wear intensity J at each stage of the experiments was determined as the ratio of the value of linear wear Δh to the friction path L, i.e.,

$$J = \Delta h / L, \quad (1)$$

The amount of linear wear Δh was determined by the formula:

$$\Delta h = \Delta G / (\rho \times F), \quad (2)$$

where ΔG is the mass loss of the specimen at this stage of testing, mg; ρ is the density of the material, kg/m^3; and F is the surface area friction of the specimen, mm^2.

The temperature in the contact zone was determined using a thermocouple, which was installed in a hole near the contact surface of the counter-specimen (cast iron specimens, immoveable).

3. Results

Metallographic studies have shown that during TDT using a tool-SWS of the flat face surfaces of specimens made of steel 41Cr4 (QH and LTT), the thickness of the reinforced layer was 150–160 μm, and the microhardness was 8.1 GPa (Figures 4 and 5). The microhardness of the base metal was 5.1 GPa. When using a tool-TG during TDT, the thickness of the reinforced layer increased to 260–280 μm, and its hardness increased to 9.7 GPa (three measurements were performed and the mean value, measurement errors, and plotting were determined in OriginPro).

In the process of strengthening by the TDT using a tool-TG, the metal of the surface layer of the workpiece in the tool-part contact zone is deformed with greater intensity. This leads to an increase in the thickness and microhardness of the reinforced layer and a decrease in grain size. The grain size is 9–11 nm near the treated surface [48]. The structure of the reinforced layers is nanocrystalline. The grain size increases with the depth of the strengthened layer.

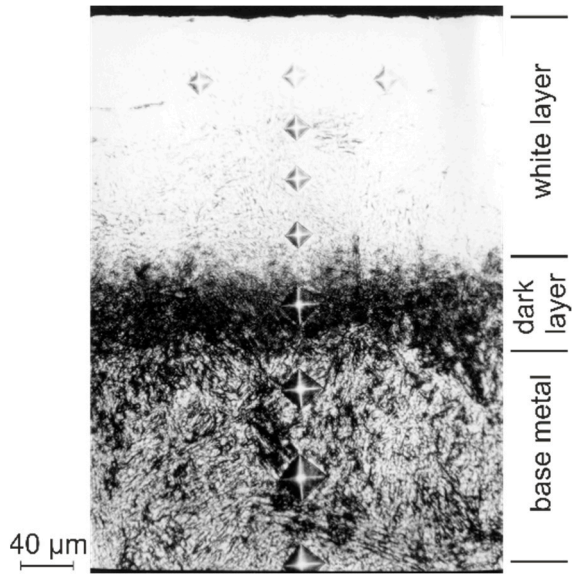

Figure 4. Microstructure of the reinforced layer after TDT of Steel 41Cr4 (QH and LTT).

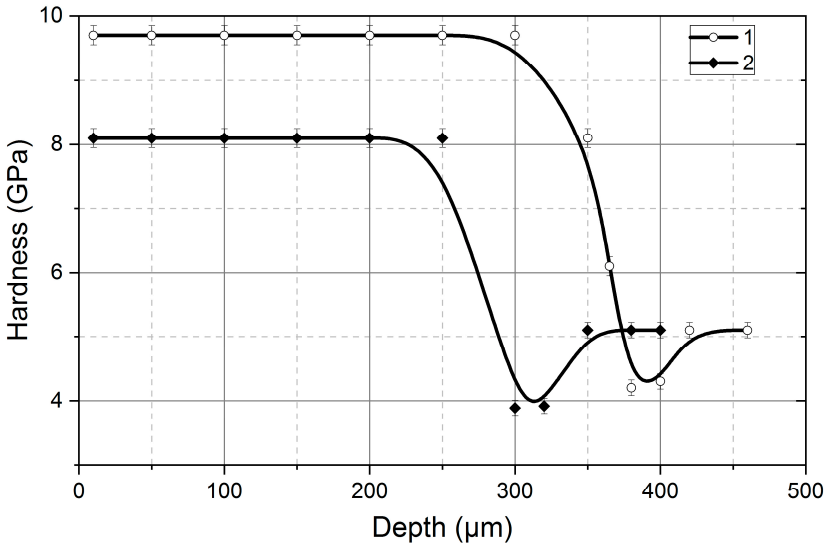

Figure 5. Microhardness of the strengthened layer after TDT of Steel 41Cr4 (QH and LTT) using the tool with a different form of a working part: 1—tool-TG; 2—tool-SWS.

During friction without lubrication, the properties of the materials directly involved in the process and those related to wear resistance are most evident. The contacting surfaces of the friction parts act on each other, and the protrusions (peaks) of both surfaces come into direct contact. Energy is localized in the contact zone, which affects the chemical and tribochemical reactions that occur on the contacting surfaces. At the same time, secondary structures are formed on them, which are different in chemical composition and structure from the contacting metals of the friction pair parts. They consist mainly of iron oxides and in most cases have a favourable effect on wear processes. High-quality, solid secondary structures generally prevent the contacting surfaces of the friction pair from adhering to each other. In cases where the rate of the formation of secondary structures is higher than the rate of their destruction, the value of the friction coefficient is reduced, and the wear rate of the friction pair is reduced too.

Experiments have shown that when a steel 41Cr4 specimen is reinforced (QH and LTT) using both tools, the wear resistance without the lubrication of the steel 41Cr4—grey cast iron EN-GJL-200 (EN) pair increases significantly.

The maximum effect of increasing the wear resistance of the friction pair after TDT compared to not reinforced specimens is at sliding velocities of 0.8–1.0 m/s, and is equal to 3.2–4.3 times (Figure 6). As the sliding velocity increases to 0.8–1.0 m/s, the formation of the type of oxides that are an integral part of the secondary structures' changes and the thickness of the oxide film decreases. The oxide film has a small thickness and is quickly destroyed. The wear rate of the film exceeds the rate of its formation, and an intensive destruction of the unprotected base metal occurs. The protrusions are cut off and solid particles of wear products are formed, which enter the friction zone as an abrasive, increasing the wear of the friction pair. The rate of the oxide film formation increases with the subsequent increase in the sliding velocity.

Only the moving specimen was strengthened. With an increase in sliding velocity (more than 1 m/s), the wear rate decreases and has a wave-like character.

The nature of the wear curves of the specimens with a white layer is the same as that of the not reinforced pair, but the wear intensity is lower. As already noted, the maximum effect is observed in the range of sliding velocities in which abrasive wear processes take place. The white layer has a higher hardness, toughness, and strength, and is therefore less susceptible to fracture.

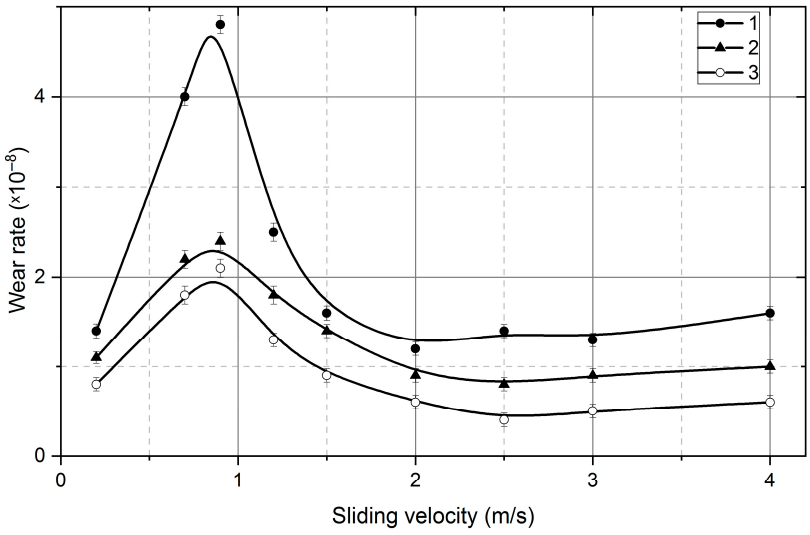

(**a**)

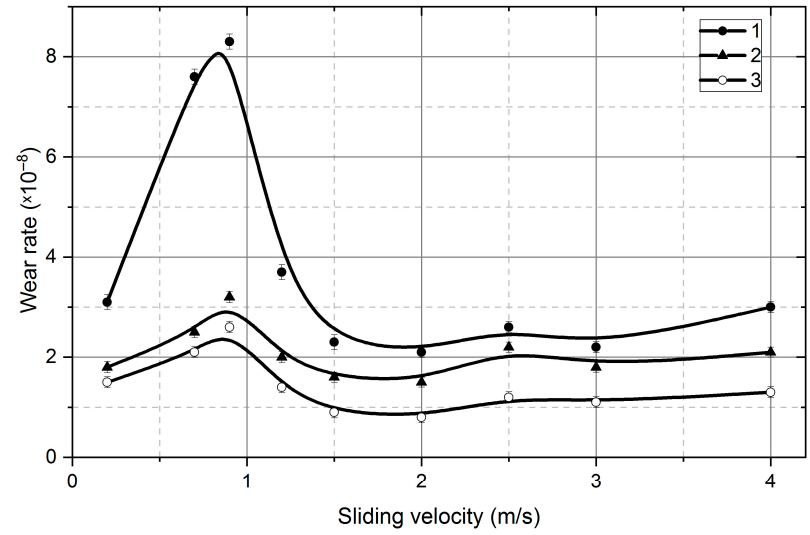

(**b**)

Figure 6. The intensity of wear of the specimen (**a**) and counter-specimen (**b**) dependence of the sliding velocity during friction without lubrication of pair Steel 41Cr4 (QH and LTT)—Grey Cast Iron EN-GJL-200 (EN) after TDT (P = 1 MPa): 1—not reinforced specimens; 2—TDT, using the tool-SWS; 3—TDT, using the tool-TG.

Significant amounts of oxides (up to 30%) were detected in the white layer with a thickness of less than 1 μm by Mössbauer spectroscopy. The reinforced surface has favourable conditions for the formation of high-quality secondary structures in the contact zone of the friction pair under different friction conditions, which significantly affect the wear process. Local X-ray diffraction studies of the white layer showed the presence of sulphur, nitrogen, chlorine, sodium, and other elements near the surface.

The quality of the reinforced white layer significantly affects the friction and wear processes. Thus, during friction, a pair in which the specimen is reinforced by a tool-TG has a lower wear rate than the same pair where the specimen is reinforced by a tool -SWS. The wear rate does not change significantly with an increase in sliding velocity.

The wear rate of the not reinforced grey cast iron specimens working in conjunction with the reinforced specimens also decreased. The effect of increasing the wear resistance is reduced in the case of the TDT of both parts of the friction pair. The TDT increases the

wear resistance of the friction pair as a whole. The white layer produced by TDT with a tool-TG increases the wear resistance compared to the white layer produced by a tool-SWS.

One of the major parameters in the wear process is the temperature in the friction zone. An increase in the temperature in the friction zone can lead to local softening, metal melting, and then adhesion. In practice, there are cases when, under severe friction conditions, the welding (adhesion) of one part to another occurs after the load is removed. Such a case can be accompanied by jamming and an accident.

When friction occurs without the lubrication of a steel 41Cr4—grey cast iron EN-GJL-200 (EN) pair, the temperature rises sharply at the beginning of the friction process, reaches a maximum after 15–20 min, and then stabilizes (Figure 7). The maximum value of the steady-state temperature in the friction zone was recorded on the ground specimens, and the minimum value was recorded after TDT with a tool-TG. The temperature in the contact zone increases with an increase in the unit load and sliding velocity (Figure 8).

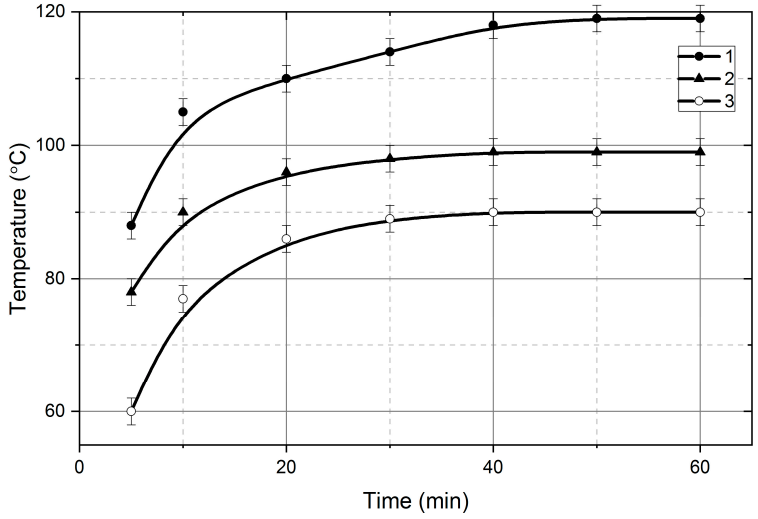

Figure 7. The kinetics of temperature in the contact zone due to friction without lubrication of pair "Steel 41Cr4 (QH and LTT)—Grey Cast Iron EN-GJL-200 (EN)" after TDT (P = 1 MPa): 1—not strengthened; 2—TDT, using the tool-SWS; 3—TDT, using the tool-TG.

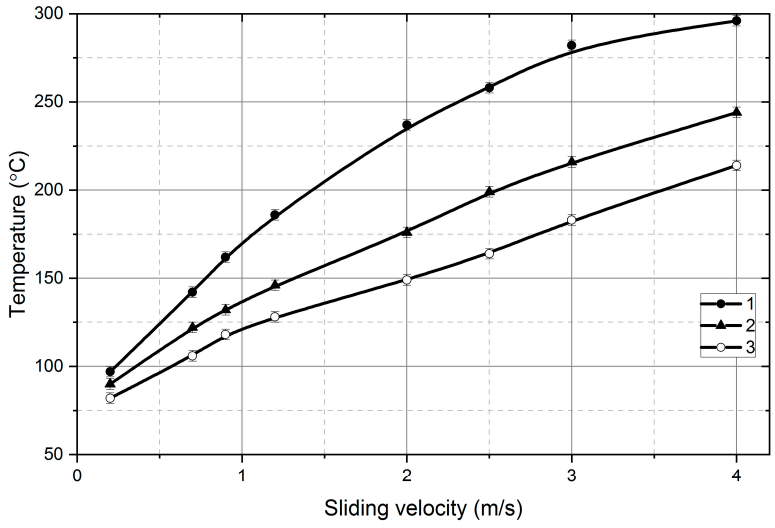

Figure 8. The dependence of the contact zone temperature on the sliding velocity due to friction without lubrication of pair "Steel 41Cr4 (quench-hardening and low-temperature tempering)—Grey Cast Iron EN-GJL-200 (EN)" after TDT (P = 1 MPa): 1—not reinforced; 2—TDT, using the tool-SWS; 3—TDT, using the tool-TG.

The coefficient of friction is also significantly affected by surface reinforcement. In the initial period of pair friction, the value of the friction coefficient increases sharply and reaches its maximum value, then the friction process stabilizes, and the friction coefficient decreases slightly (Figure 9).

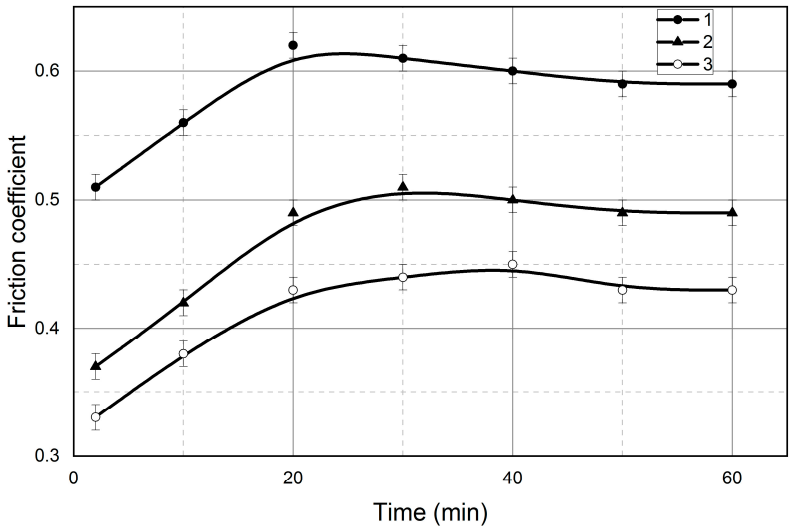

Figure 9. The kinetics of friction coefficient in the contact zone due to friction without lubrication of pair "Steel 41Cr4 (QH and LTT)—Grey Cast Iron EN-GJL-200 (EN)" after TDT (P = 1 MPa): 1—not reinforced; 2—TDT, using the tool-SWS; 3—TDT, using the tool-TG.

During this time, secondary structures are formed on the surfaces of the friction pair. The structural adaptability of this friction pair occurs, which leads to the establishment of the value of the friction coefficient. The coefficient of friction in the initial period increases since the contacting surfaces of the pair do not adjoin the entire area, and at certain points and contact spots, a high unit load occurs, and, accordingly, the temperature increases.

The friction surfaces are smoothed and high-quality secondary structures are formed if the force required to shift the individual points of the contacting parts is less than the intermolecular adhesion force. The metal is torn from the surface, and accidental wear is possible if the forces of interatomic adhesion are lower.

The decrease in the friction coefficient with an increase in the unit load can be explained by the more intense oxidation processes. Increasing pressure increases the temperature in the contact zone, which contributes to the formation of high-quality secondary structures, which in turn reduces the role of adhesion. The kinetics of the friction coefficient of the steel-iron pair can be explained by the different physical and mechanical properties of the materials, and especially by the presence of graphite in the cast iron, which is released into the friction zone (Figure 10).

At low sliding velocities, the friction coefficient has maximum values. With an increase in sliding velocity, the friction coefficient first decreases and then increases again, reaches a peak, and then decreases monotonically (Figure 11).

If we compare the dependence of the wear intensity and friction coefficient, the highest value of the coefficient corresponds to the sliding velocity at which the shape of iron oxide changes in secondary structures.

Oxidative wear can be divided into several stages: the adsorption and diffusion of oxygen on the friction surface, and the formation of secondary structures and their destruction. The adsorption and diffusion of oxygen on the surface and in the surface layers of the friction pair are the main factors that affect the properties of secondary structures. As a result of repeated loading and the presence of internal stresses, microcracks appear and develop in secondary structures, the bonds weaken, and the films delaminate at the interface between the secondary structures and the base metal. The time required

for the destruction of the oxide film depends on the strength of its adhesion to the base metal and the contact stresses in the contact zone. The higher the adhesion, the lower the ratio of the specific volumes of the oxide and the base metal: for FeO, this ratio is 1.72; for Fe_2O_3—2.15; and for Fe_3O_4—2.1. At low contact loads and low sliding velocities, secondary structures mainly consist of Fe_2O_3 oxide, and under more severe friction conditions—of Fe_3O_4 [50,51].

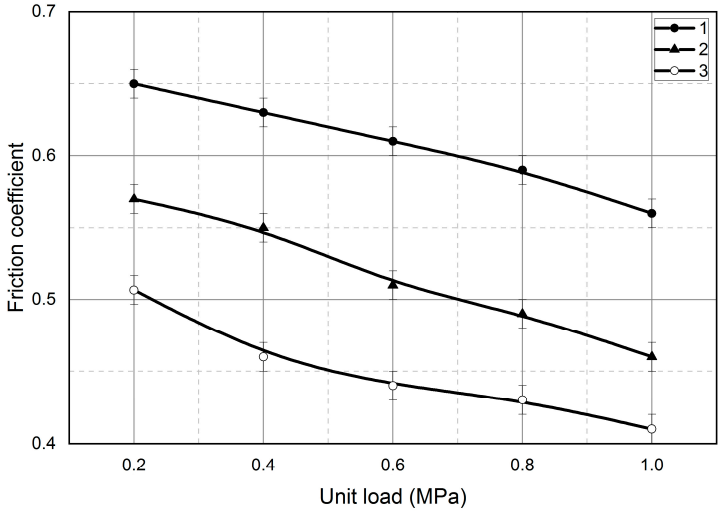

Figure 10. The friction coefficient dependence of the unit load during process of friction without lubrication of pair "Steel 41Cr4 (QH and LTT)—Grey Cast Iron EN-GJL-200 (EN)" after TDT (P = 1 MPa): 1—not reinforced; 2—TDT, using the tool-SWS; 3—TDT, using the tool-TG.

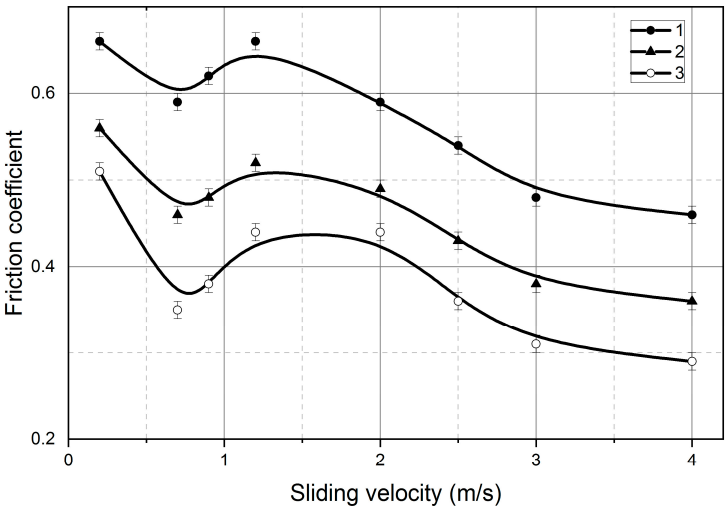

Figure 11. The friction coefficient dependence of the sliding velocity during the process of friction without lubrication of pair "Steel 41Cr4 (QH and LTT)—Grey Cast Iron EN-GJL-200 (EN)" after TDT (P = 1 MPa): 1—not strengthened; 2—TDT, using the tool-SWS; 3—TDT, using the tool-TG.

The sliding velocity significantly affects the thermal operation of the contact and the type of oxide film. At low sliding velocities, only the Fe_2O_3 film wears out, since its thickness is higher than the critical one, i.e., the rate of film formation is higher than the rate of its destruction. With an increase in sliding velocity, the Fe_2O_3 film and the base metal wear, with the latter wearing much faster than the film. As the sliding velocity increases, the temperature at the surface of the contacting bodies reaches values at which Fe_3O_4 oxide appears and wear begins, partly affecting the base metal. With a further increase in sliding velocity, only the wear of the Fe_3O_4 film is observed.

The kinetics of mechanical and chemical wear depend heavily on processes that take place in very thin layers under the influence of high local temperatures, pressures, and strains. These high-speed processes lead to changes in the chemical composition of surface layers. One of the mechanisms for accumulating energy supplied to a metal during its mechanical deformation is its accumulation in the form of dislocation energy. This energy, in our opinion, mainly ensures the occurrence of tribochemical reactions in the contact zone during friction pair wear. Much of the mechanical work consumed in the friction process is converted into heat, which is constantly removed from the friction zone by heat conduction, convection, or radiation. The dislocation energy is concentrated in the thin surface layer and is an important source for these chemical reactions.

The reinforced nanocrystalline white layer has an increased density of dislocations (more than 10 times) and an increased amount of residual austenite compared to the main structure [48,52]. The dispersion of martensite, residual austenite, and carbides in the white layer is much higher than in steel after quench-hardening and low-temperature tempering. The residual austenite increases the viscosity of the surface layer while increasing its hardness due to the high dispersion of martensite. In this case, the resistance to plastic deformation also increases. The increased number of dislocations activates the surface, increases the rate of diffusion and chemical reactions, and accelerates the formation of oxide films. At the same time, the dislocations in the white layer are blocked, their movement is impaired, and crack initiation is inhibited, which means that the formation of wear products is reduced.

The main field of application is sliding bearings, where the shaft is made of steel, and the insert is made of cast iron.

4. Conclusions

In the TDT process, the surface layers of the specimens made of 41Cr4 steel (QH and LTT) are subjected to the formation of reinforced layers with an NCS. The thickness of the reinforced layer was 150–160 μm and the microhardness was 8.1 GPa when the tool-SWS was used. The microhardness of the base metal was 5.1 GPa. When using a tool-TG during TDT, the thickness of the reinforced layer increased to 260–280 μm, and the hardness increased to 9.7 GPa. The structure of the reinforced layer is nanocrystalline.

After the TDT of the contact surfaces of specimens made of steel 41Cr4 with a tool-TG, the wear resistance of the friction pair steel 41Cr4—grey cast iron EN-GJL-200 (EN) increased by 2.2–2.3 times compared to the not reinforced pair at a sliding velocity of 0.8–1.0 m/s.

With an increase in sliding velocity from 0.25 m/s to 4 m/s, the temperature in the friction zone increases monotonically. The lowest temperature occurs during the sliding of the friction pair with the specimen with a reinforced layer by the tool-TG and is ~60 °C at a velocity of 0.25 m/s and ~220 °C at 4 m/s. During the sliding of a not reinforced friction pair, the temperature is ~100 °C and ~300 °C, respectively.

The lowest value of the friction coefficient was obtained when the friction pair slid against the reinforced specimen with the tool-TG. The nature of the change in the friction coefficient is similar to the change in the wear intensity of the friction pair, and is ~0.5 at a velocity of 0.25 m/s and ~0.3 at 4 m/s.

The study of steel-iron friction pairs under friction without lubrication has shown that white layers reinforced with NCS significantly increase the resistance to wear.

Author Contributions: Conceptualization, V.G. and I.H.; methodology, I.H., V.G., A.A. and P.M.; validation, I.H., P.M., O.P. and A.F.; formal analysis, I.H., P.M., A.A., A.F., V.G. and V.D.; investigation, I.H., V.G., A.A., A.F., P.M. and O.P.; writing—original draft preparation, I.H., P.M., A.A., A.F., V.G. and V.D.; writing—review and editing, I.H., P.M., A.A., A.F., V.G., V.D. and O.P.; visualization, V.G. and I.H.; supervision, I.H. and P.M. All authors have read and agreed to the published version of the manuscript.

Funding: This research received no external funding.

Data Availability Statement: The data presented in this study are available upon request from the corresponding author.

Acknowledgments: We gratefully acknowledge funding in the form of EU Grant No: [2017-1-UK01-KA107-036029], which permitted this collaborative work to take place.

Conflicts of Interest: The authors declare no conflict of interest.

References

1. Dwivedi, D.K. Surface Engineering. In *Enhancing Life of Tribological Components*; Springer: New Delhi, India, 2018; ISBN 978-81-322-3777-8.
2. Totten, G.E. *Encyclopedia of Iron, Steel, and Their Alloys (Online Version)*; Totten, G.E., Colas, R., Eds.; CRC Press: Boca Raton, FL, USA, 2016; ISBN 9781000031676.
3. Santecchia, E.; Hamouda, A.M.S.; Musharavati, F.; Zalnezhad, E.; Cabibbo, M.; El Mehtedi, M.; Spigarelli, S. A Review on Fatigue Life Prediction Methods for Metals. *Adv. Mater. Sci. Eng.* **2016**, *2016*, 9573524. [CrossRef]
4. Hutchings, I.; Shipway, P. *Tribology: Friction and Wear of Engineering Materials*, 2nd ed.; Butterworth-Heinemann: Oxford, UK, 2017; ISBN 9780081009109.
5. Sethuramiah, A.; Kumar, R. *Modeling of Chemical Wear*; Elsevier: Amsterdam, The Netherlands, 2015; ISBN 9780128045336.
6. Hirani, H. *Fundamentals of Engineering Tribology with Applications*; Cambridge University Press: Cambridge, UK, 2016; ISBN 9781107063877.
7. Davis, J.R. *Surface Engineering for Corrosion and Wear Resistance*; Davis, J.R., Ed.; ASM International: Detroit, MI, USA, 2001; ISBN 978-1-62708-315-7.
8. Quintino, L. Overview of Coating Technologies. In *Surface Modification by Solid State Processing*; Elsevier: Amsterdam, The Netherlands, 2014; pp. 1–24. ISBN 9780857094681.
9. Yushchenko, K.A.; Borysov, Y.S.; Kuznetsov, V.D.; Korzh, V.M. *Surface Engineering*; Naukova Dumka: Kyiv, Ukraine, 2007.
10. Holmberg, K.; Matthews, A. Tribology of Engineered Surfaces. In *Wear—Materials, Mechanisms and Practice*; Wiley: Hoboken, NJ, USA, 2005; pp. 123–166.
11. Wu, L.; Guo, X.; Zhang, J. Abrasive Resistant Coatings—A Review. *Lubricants* **2014**, *2*, 66–89. [CrossRef]
12. Mang, T.; Bobzin, K.; Bartels, T. *Industrial Tribology*, 1st ed.; Wiley-VCH: Hoboken, NJ, USA, 2011; ISBN 9783527632596.
13. Oborskyi, G.; Orgiyan, A.; Ivanov, V.; Balaniuk, A.; Pavlenko, I.; Trojanowska, J. Improvement of the Dynamic Quality of Cantilever Boring Bars for Fine Boring. *Machines* **2022**, *11*, 7. [CrossRef]
14. Dzyura, V.; Maruschak, P. Optimizing the Formation of Hydraulic Cylinder Surfaces, Taking into Account Their Microrelief Topography Analyzed during Different Operations. *Machines* **2021**, *9*, 116. [CrossRef]
15. Kalchenko, V.; Yeroshenko, A.; Boyko, S. Crossing Axes of Workpiece and Tool at Grinding of the Circular Trough with Variable Profile. *Acta Mech. Autom.* **2018**, *12*, 281–285. [CrossRef]
16. Kalchenko, V.V.; Yeroshenko, A.M.; Boyko, S.V.; Ignatenko, P.L. Development and Research of Thermoplastic Methods for Hardening Details. *Nauk. Visnyk Natsionalnoho Hirnychoho Universytetu* **2020**, *2*, 53–60. [CrossRef]
17. Bazaluk, O.; Dubei, O.; Ropyak, L.; Shovkoplias, M.; Pryhorovska, T.; Lozynskyi, V. Strategy of Compatible Use of Jet and Plunger Pump with Chrome Parts in Oil Well. *Energies* **2021**, *15*, 83. [CrossRef]
18. Protsenko, V.S.; Bobrova, L.S.; Danilov, F.I. Effects of Water and Sodium Dodecyl Sulfate Additives on Cr(III) Ions Electroreduction in a Deep Eutectic Solvent. *Vopr. Khimii I Khimicheskoi Tekhnologii* **2021**, *2*, 110–116. [CrossRef]
19. Dutkiewicz, M.; Velychkovych, A.; Shatskyi, I.; Shopa, V. Efficient Model of the Interaction of Elastomeric Filler with an Open Shell and a Chrome-Plated Shaft in a Dry Friction Damper. *Materials* **2022**, *15*, 4671. [CrossRef]
20. Bembenek, M.; Prysyazhnyuk, P.; Shihab, T.; Machnik, R.; Ivanov, O.; Ropyak, L. Microstructure and Wear Characterization of the Fe-Mo-B-C—Based Hardfacing Alloys Deposited by Flux-Cored Arc Welding. *Materials* **2022**, *15*, 5074. [CrossRef]
21. Ropyak, L.; Shihab, T.; Velychkovych, A.; Dubei, O.; Tutko, T.; Bilinskyi, V. Design of a Two-Layer Al–Al_2O_3 Coating with an Oxide Layer Formed by the Plasma Electrolytic Oxidation of Al for the Corrosion and Wear Protections of Steel. *Prog. Phys. Met.* **2023**, *24*, 319–365. [CrossRef]
22. Lukaszkowicz, K. Review of Nanocomposite Thin Films and Coatings Deposited by PVD and CVD Technology. In *Nanomaterials*; Rahman, M.M., Ed.; InTech: London, UK, 2011.
23. Huang, X.; Ren, Y.; Zhou, Z.; Xiao, H. Experimental Study on White Layers in High-Speed Grinding of AISI52100 Hardened Steel. *J. Mech. Sci. Technol.* **2015**, *29*, 1257–1263. [CrossRef]
24. Olugbade, T.O.; Lu, J. Literature Review on the Mechanical Properties of Materials after Surface Mechanical Attrition Treatment (SMAT). *Nano Mater. Sci.* **2020**, *2*, 3–31. [CrossRef]
25. Klocke, F.; Hensgen, L.; Klink, A.; Ehle, L.; Schwedt, A. Structure and Composition of the White Layer in the Wire-EDM Process. *Procedia CIRP* **2016**, *42*, 673–678. [CrossRef]
26. Bartkowska, A. Production and Properties of FeB-Fe_2B-Fe_3(B,C) Surface Layers Formed on Tool Steel Using Combination of Diffusion and Laser Processing. *Coatings* **2020**, *10*, 1130. [CrossRef]
27. Korzhyk, V.; Tyurin, Y.; Kolisnichenko, O. *Theory and Practice of Plasma-Detonation Technology of Surface Hardening Metal Products*; Privat Company Technology Center: Kharkiv, Ukraine, 2021; ISBN 9786177319466.

28. Vilaça, P. Friction Surfacing. In *Surface Modification by Solid State Processing*; Elsevier: Amsterdam, The Netherlands, 2014; pp. 25–72.
29. Nykyforchyn, H.; Kyryliv, V.; Maksymiv, O. Wear Resistance of Steels with Surface Nanocrystalline Structure Generated by Mechanical-Pulse Treatment. *Nanoscale Res. Lett.* **2017**, *12*, 150. [CrossRef]
30. Javaheri, V.; Sadeghpour, S.; Karjalainen, P.; Lindroos, M.; Haiko, O.; Sarmadi, N.; Pallaspuro, S.; Valtonen, K.; Pahlevani, F.; Laukkanen, A.; et al. Formation of Nanostructured Surface Layer, the White Layer, through Solid Particles Impingement during Slurry Erosion in a Martensitic Medium-Carbon Steel. *Wear* **2022**, *496–497*, 204301. [CrossRef]
31. Cappellini, C.; Attanasio, A.; Rotella, G.; Umbrello, D. Formation of White and Dark Layers in Hard Cutting: Influence of Tool Wear. *Int. J. Mater. Form.* **2010**, *3*, 455–458. [CrossRef]
32. Hosseini, S.B.; Klement, U. A Descriptive Phenomenological Model for White Layer Formation in Hard Turning of AISI 52100 Bearing Steel. *CIRP J. Manuf. Sci. Technol.* **2021**, *32*, 299–310. [CrossRef]
33. Gleiter, H. Nanostructured Materials: Basic Concepts and Microstructure. *Acta Mater.* **2000**, *48*, 1–29. [CrossRef]
34. Zhang, F.; Duan, C.; Wang, M.; Sun, W. White and Dark Layer Formation Mechanism in Hard Cutting of AISI52100 Steel. *J. Manuf. Process.* **2018**, *32*, 878–887. [CrossRef]
35. Pan, R.; Chen, Y.; Lan, H.; Shiju, E.; Ren, R. Investigation into the Evolution of Tribological White Etching Layers. *Mater. Charact.* **2022**, *190*, 112076. [CrossRef]
36. Harsha, R.N.; Mithun Kulkarni, V.; Satish Babu, B. Severe Plastic Deformation—A Review. *Mater. Today Proc.* **2018**, *5*, 22340–22349. [CrossRef]
37. Valiev, R.; Islamgaliev, R.; Alexandrov, I. Bulk Nanostructured Materials from Severe Plastic Deformation. *Prog. Mater. Sci.* **2000**, *45*, 103–189. [CrossRef]
38. Segal, V.M. Deformation Mode and Plastic Flow in Ultra Fine Grained Metals. *Mater. Sci. Eng. A* **2005**, *406*, 205–216. [CrossRef]
39. Lowe, T.C.; Zhu, Y.T.; Semiatin, S.L.; Berg, D.R. Overview and Outlook for Materials Processed by Severe Plastic Deformation. In *Investigations and Applications of Severe Plastic Deformation*; Lowe, T.C., Valiev, R.Z., Eds.; Springer: Dordrecht, The Netherlands, 2000; pp. 347–356. ISBN 978-94-011-4062-1.
40. Hahn, H. Unique Features and Properties of Nanostructured Materials. In *Nanomaterials by Severe Plastic Deformation*; Wiley-VCH Verlag GmbH & Co. KGaA: Weinheim, Germany, 2005; pp. 2–17. ISBN 9783527602469.
41. Kyryliv, V.I.; Gurey, V.I.; Maksymiv, O.V.; Hurey, I.V.; Kulyk, Y.O. Influence of the Deformation Mode on the Force Conditions of Formation of the Surface Nanostructure of 40Kh Steel. *Mater. Sci.* **2021**, *57*, 422–427. [CrossRef]
42. Gurey, V.; Hurey, I. The Effect of the Hardened Nanocrystalline Surface Layer on Durability of Guideways. In Proceedings of the Lecture Notes in Mechanical Engineering, Hammamet, Tunisia, 20–22 December 2021; Tonkonogyi, V., Ivanov, V., Trojanowska, J., Oborskyi, G., Edl, M., Kuric, I., Pavlenko, I., Dasic, P., Eds.; Springer International Publishing: Cham, Switzerland, 2020; pp. 63–72.
43. Hurey, I.; Hurey, T.; Gurey, V. Wear Resistance of Hardened Nanocrystalline Structures in the Course of Friction of Steel-Grey Cast Iron Pair in Oil-Abrasive Medium. In Proceedings of the Lecture Notes in Mechanical Engineering, Hammamet, Tunisia, 20–22 December 2021; Ivanov, V., Trojanowska, J., Machado, J., Liaposhchenko, O., Zajac, J., Pavlenko, I., Edl, M., Perakovic, D., Eds.; Springer International Publishing: Cham, Switzerland, 2020; pp. 572–580.
44. Gurey, V.; Hurey, I. Influence of Surface Hardened Nanocrystalline Layers on the Resistance of Contact Fatigue Destruction. In Proceedings of the Lecture Notes in Mechanical Engineering, Hammamet, Tunisia, 20–22 December 2021; Ivanov, V., Trojanowska, J., Pavlenko, I., Zajac, J., Peraković, D., Eds.; Springer International Publishing: Cham, Switzerland, 2020; pp. 483–491.
45. Gurey, V.; Shynkarenko, H.; Kuzio, I. Mathematical Model of the Thermoelasticity of the Surface Layer of Parts During Discontinuous Friction Treatment. *Lect. Notes Mech. Eng.* **2021**, *1*, 12–22. [CrossRef]
46. Gurey, V.; Maruschak, P.; Hurey, I.; Dzyura, V.; Hurey, T.; Wojtowicz, W. Dynamic Analysis of the Thermo-Deformation Treatment Process of Flat Surfaces of Machine Parts. *J. Manuf. Mater. Process* **2023**, *7*, 101. [CrossRef]
47. Hurey, I.; Hurey, T.; Lanets, O.; Dmyterko, P. The Durability of the Nanocrystalline Hardened Layer during the Fretting Wear. In *Lecture Notes in Mechanical Engineering*; Springer: Berlin/Heidelberg, Germany, 2021; pp. 23–32. [CrossRef]
48. Kyryliv, V.; Maksymiv, O.; Gurey, V.; Hurey, I.; Kyryliv, Y.; Zvirko, O. The Mode Deformation Effect on Surface Nanocrystalline Structure Formation and Wear Resistance of Steel 41Cr4. *Coatings* **2023**, *13*, 249. [CrossRef]
49. Hurei, I.V.; Hurei, T.A.; Tykhonovych, V.V. Redistribution of Chemical Elements in the Process of Pulse Strengthening. *Mater. Sci.* **1999**, *35*, 146–148. [CrossRef]
50. Tao, F.F. A Study of Oxidation Phenomena in Corrosive Wear. *ASLE Trans.* **1969**, *12*, 97–105. [CrossRef]
51. Yoshimoto, G.; Tsukizoe, T. On the Mechanism of Wear between Metal Surfaces. *Wear* **1958**, *1*, 472–490. [CrossRef]
52. Khitouni, N.; Hammami, B.; Llorca-Isern, N.; Ben Mbarek, W.; Suñol, J.-J.; Khitouni, M. Microstructure and Magnetic Properties of Nanocrystalline Fe60−xCo25Ni15Six Alloy Elaborated by High-Energy Mechanical Milling. *Materials* **2022**, *15*, 6483. [CrossRef] [PubMed]